

Pharmacokinetics, Pharmacodynamics, Safety, and Tolerability of Oral Venglustat in Healthy Volunteers

Clinical Pharmacology
in Drug Development
2021, 10(1) 86–98
© 2020 The Authors. *Clinical Pharmacology in Drug Development*
published by Wiley Periodicals LLC
on behalf of American College of
Clinical Pharmacology
DOI: 10.1002/cpdd.865

M. Judith Peterschmitt¹, Nigel P. S. Crawford^{2,*}, Sebastiaan J. M. Gaemers³,
Allena J. Ji⁴, Jyoti Sharma², and Theresa T. Pham⁵

Abstract

Venglustat is a small-molecule glucosylceramide synthase (GCS) inhibitor designed to reduce the production of glucosylceramide (GL-1) and thus is expected to substantially reduce formation of glucosylceramide-based glycosphingolipids. Because of its effect on glycosphingolipid formation, GCS inhibition has therapeutic potential across many disorders affecting glycosphingolipid metabolism. Therefore, venglustat is under development for substrate reduction therapy in multiple diseases, including Gaucher disease type 3, Parkinson's disease associated with *GBA* mutations, Fabry disease, GM2 gangliosidosis, and autosomal dominant polycystic kidney disease. Phase I studies were conducted in healthy volunteers to determine venglustat pharmacokinetics, pharmacodynamics, safety, and tolerability and to assess food effects on pharmacokinetics (single-dose and food-effect studies: NCT01674036; repeated-dose study: NCT01710826). Following a single oral dose of venglustat L-malate (2, 5, 15, 25, 50, 100, or 150 mg), venglustat demonstrated linear pharmacokinetics, rapid absorption (median t_{max} , 3.00–5.50 hours), systemic exposure unaffected by food, low apparent total body clearance (mean CL/F, 5.18–6.43 L/h), and pooled geometric mean $t_{1/2z}$ of 28.9 hours. Following repeated once-daily oral doses of venglustat L-malate (5, 10, or 20 mg) for 14 days, apparent steady state occurred within 5 days of repeated dosing, with pooled accumulation ratios of 2.10 for C_{max} and 2.22 for AUC_{0-24} , and no statistically significant effect of dose or sex on accumulation. The mean fraction of dose excreted unchanged in urine (fe_{0-24}) was 26.3% to 33.1%. Plasma GL-1 and GM3 decreased time- and dose-dependently. Venglustat demonstrated a favorable safety and tolerability profile.

Keywords

glucosylceramide (GL-1), globotriaosylceramide (GL-3), glucosylceramide synthase (GCS) inhibition, glucosylsphingosine (lyso-GL-1), monosialodihexosylganglioside (GM3), substrate reduction therapy, venglustat (GZ/SAR402671; Genz-682452)

Glycosphingolipids are essential for diverse cellular functions, and abnormalities of glycosphingolipid metabolism can have important consequences for health and disease.^{1,2} Glucosylceramide (GL-1), formed from ceramide and uridine diphosphate-glucose by glucosylceramide synthase (GCS), is the central building block for more complex glycosphingolipids such as globotriaosylceramide (GL-3), monosialodihexosylganglioside (GM3), disialotetrahexosylganglioside (GM2), and monosialotetrahexosylganglioside (GM1 ganglioside).³ Inherited deficiencies of enzymes acting on substrates downstream of GCS can cause severe glycosphingolipid metabolic dysregulation in Gaucher disease (GD),⁴ Fabry disease (FD),⁵ and GM2 gangliosidosis,⁶ as well as in Parkinson's disease in patients carrying *GBA* mutations (*GBA*-PD).⁷ GL-1 and GM3 dysregulation also

¹Sanofi Genzyme, Cambridge, Massachusetts, USA

²Sanofi, Bridgewater, New Jersey, USA

³Sanofi Genzyme, Amsterdam, The Netherlands

⁴Sanofi Genzyme, Framingham, Massachusetts, USA

⁵PPD Development, LLC, Austin, Texas, USA

This is an open access article under the terms of the Creative Commons Attribution-NonCommercial-NoDerivs License, which permits use and distribution in any medium, provided the original work is properly cited, the use is non-commercial and no modifications or adaptations are made.

Submitted for publication 6 January 2020; accepted 26 July 2020.

Corresponding Author:

M. Judith Peterschmitt, MD, MMSc, Sanofi Genzyme, 50 Binney Street, Cambridge, MA 02142
(e-mail: Judith.Peterschmitt@sanofi.com)

*At the time the studies were conducted. Current affiliation: Daiichi Sankyo, Inc., Basking Ridge, New Jersey, USA

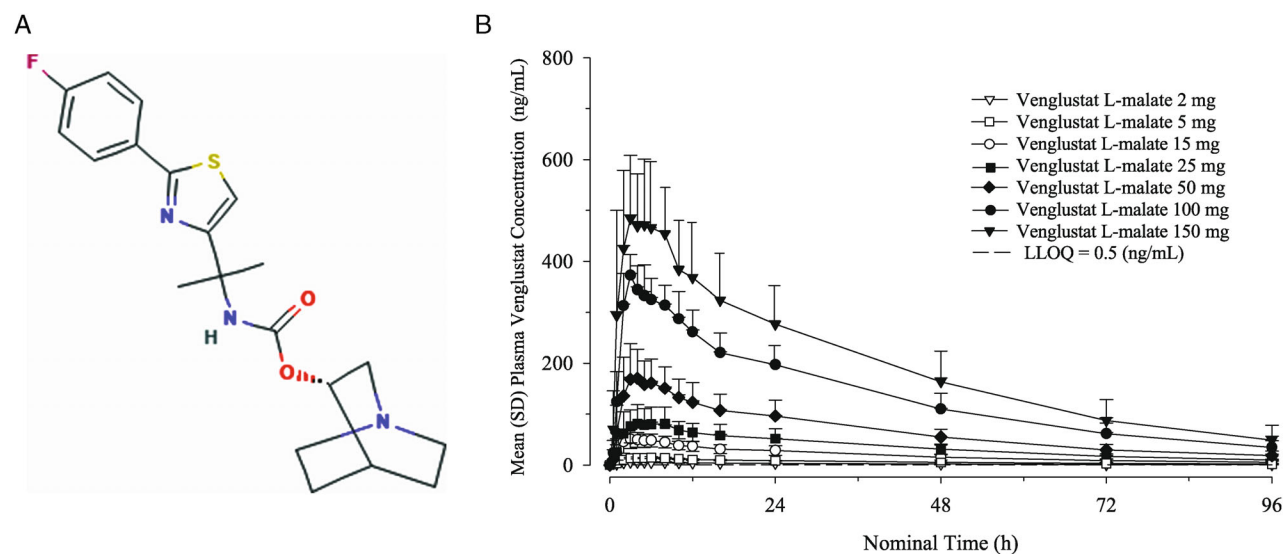


Figure 1. (A) Structure of venglustat, [(3S)-1-azabicyclo[2.2.2]octan-3-yl] N-[2-[2-(4-fluorophenyl)-1,3-thiazol-4-yl]propan-2-yl]carbamate (PubChem CID 60199242; National Center for Biotechnology Information. PubChem Database. Venglustat, CID=60199242, <https://pubchem.ncbi.nlm.nih.gov/compound/Venglustat#section=2D-Structure> [accessed on March 13, 2020]). (B) Mean (+ standard deviation) venglustat plasma concentrations in the single ascending-dose study. Values below the lower limit of quantitation (LLOQ) were considered zero for this graph.

occurs in autosomal dominant polycystic kidney disease (ADPKD) as GCS activity increases, resulting in pathogenic glycosphingolipid accumulation.^{1,8–11} In all these cases, GCS inhibition may provide therapeutic benefit by reducing formation of the upstream glycosphingolipid building block GL-1.¹²

Substrate reduction therapy (SRT) relies on small-molecule inhibition of an upstream enzyme to reduce pathogenic substrate accumulation. Clinical precedent exists for SRT of a glycosphingolipid-related disorder by GCS inhibition.¹² For example, eliglustat, an oral GCS inhibitor, is approved as first-line therapy for adults with GD type 1 with extensive, intermediate, or poor cytochrome P450 (CYP) 2D6-metabolizer phenotypes.¹³ However, eliglustat is subject to *P*-glycoprotein-mediated efflux from the blood-brain barrier,¹⁴ making it unsuitable for treatment of overt central nervous system (CNS) manifestations in neuronopathic (types 2 and 3) GD, GM2 gangliosidosis, or *GBA*-PD. Sanofi Genzyme is developing venglustat (GZ/SAR402671, PubChem CID 60199242; Figure 1A), a novel brain-penetrant GCS inhibitor, as an investigational disease-modifying therapy for multiple disorders associated with GL-1-related glycosphingolipids. Based on nonclinical studies (absorption, distribution, metabolism, and elimination; pharmacodynamics; and disease-model efficacy) showing availability and efficacy in proposed target organs including the CNS,^{11,15–17} venglustat is under investigation for treatment of FD, ADPKD, GD type 3, *GBA*-PD, and GM2 gangliosidosis.

As determined from unpublished in vitro studies using human biomaterial, CYP3A4 was found to be the predominant (approximately 80%) drug-metabolizing CYP450 isozyme contributing to the metabolism of venglustat. Clinical significance of impact of CYP3A inhibitors and inducers on venglustat pharmacokinetics still needs to be evaluated. Further, based on in vitro CYP inhibition, CYP induction, and *P*-glycoprotein inhibition data, the likelihood for drug-drug interactions because of inhibition or induction of the major CYP450-metabolizing enzymes and inhibition of *P*-glycoprotein by venglustat is considered remote. In vitro assessment for additional potential transporter-mediated drug-drug interactions is ongoing.

Venglustat can correct the aberrant flux of glycosphingolipids, which are key pathogenic contributors in *GBA*-PD¹⁸ and ADPKD in mouse models.¹ Heterozygous *GBA* mutations are the most common genetic risk factor for Parkinson's disease and dementia with Lewy bodies,¹⁹ and lipid substrate accumulation has been reported in *GBA*-PD cultured neurons and patient brain tissue.⁷ Pharmacologic GL-1 reduction in 2 mouse models of synucleinopathies decreased α -synuclein pathology and improved behavioral outcomes, indicating that GCS inhibition can modulate α -synuclein processing and potentially reduce Parkinson's disease progression¹⁵; thus, venglustat is being studied in human *GBA*-PD.²⁰ In ADPKD, GCS-mediated glycosphingolipid accumulation contributes to cystogenesis in humans and mice. GCS inhibition has been shown to reduce cystogenesis,

improve urine concentration, and reduce the rate of renal function decline in 3 genetic models of polycystic kidney disease including the orthologous ADPKD mouse model,¹¹ supporting investigation of venglustat in ADPKD.¹ Venglustat has been shown to reduce CNS histopathological changes, improve behavioral responses, and increase life span in a mouse model of neuronopathic GD¹⁶ and is being studied in human adult GD3.¹⁸ In a mouse FD model, venglustat alone reduced GL3 accumulation and histopathologic changes and in combination with agalsidase beta augmented peripheral efficacy of enzyme replacement.¹⁷ Venglustat may in principle be applicable to treatment of GM2 gangliosidosis via its ability to reduce GM2 synthesis and CNS availability.⁶

In view of venglustat's proposed mechanism of action, preclinical pharmacology, and safety profile, phase 1 clinical studies were conducted to evaluate its pharmacokinetics, pharmacodynamics, safety, and tolerability to support future drug development. This report summarizes the results from 3 phase 1 studies in healthy volunteers (single ascending-dose study and effect of food on venglustat pharmacokinetics following a single dose, both NCT01674036, and multiple ascending-dose study NCT01710826).

Methods

Ethics and Study Designs

All 3 studies received institutional review board approvals (IntegReview, Austin, Texas), complying with the Declaration of Helsinki (1964) and applicable amendments, and were conducted according to Good Clinical Practice. All subjects gave written informed consent before participating. The studies were conducted by PPD Development, LLC, at a single center in Austin, Texas. TDU12766-FED12767 (NCT01674036) was a 2-part single-center trial in healthy adult male volunteers. Study TDU12766 was a double-blind, randomized, placebo-controlled sequential ascending single-dose study of venglustat safety, tolerability, and pharmacokinetics. Study FED12767 was an open-label, randomized, crossover 2-sequence, 2-period, 2-treatment study of venglustat pharmacokinetics with and without a high-fat meal, with a minimum 7-day washout period between treatment conditions. TDR12768 (NCT01710826) was a single-center, double-blind, randomized, placebo-controlled, sequential ascending repeated-dose study of the safety, tolerability, pharmacokinetics, and pharmacodynamics of venglustat in healthy adult male and female volunteers.

Subjects

Inclusion criteria defined eligible subjects as men (TDU12766-FED12767 and TDR12768) and women

(TDR12768 only) aged 18–45 years, weighing 50–100 kg (men) or 40–90 kg (women), with normal-range vital signs, normal 12-lead electrocardiogram (ECG) results (after 10 minutes supine), and normal laboratory parameters. Women participants had to test negative for pregnancy. Sexually active subjects and their partners (except women > 1 year postmenopausal or sterilized \geq 3 months earlier) had to use double contraception methods on-study and for 2 months after final dosing.

Key exclusion criteria included:

- History or presence of clinically relevant cardiovascular, pulmonary, gastrointestinal, hepatic, renal, metabolic, hematological, neurological, musculoskeletal, psychiatric, systemic, ocular, or infectious disease (including hepatitis B or C or human immunodeficiency virus 1 or 2), or signs of acute illness;
- Frequent headaches and/or migraines, recurrent nausea and/or vomiting;
- Blood donation (>100 mL) within 2 months before the study; symptomatic postural hypotension;
- Presence or history of drug hypersensitivity, allergic disease, or substance abuse; smoking (>5 cigarettes/day equivalent, if unable to stop on-study); any medication (including St. John's wort) within 14 days before inclusion or within 5 elimination or pharmacodynamic half-lives of study medication; any vaccination within the last 28 days; citrus fruit or juice consumption within 5 days before or during the study.

Study Drug

Venglustat L-malate (venglustat A, PubChem 60199241) and placebo were provided as capsules (venglustat L-malate: 5 mg [3.7 mg venglustat base], 25 mg, or 250 mg); 250-milligram capsules were used to prepare a solution for a 2-mg liquid dose. Starting doses were based on FDA guidance, predicted human pharmacokinetics, and the pharmacologically active dose. Dose escalation was based on adequate exposure margins from preclinical toxicology and supported by monitoring of potential safety signals and exposure (not to have exceeded 27 900 ng·h/mL, the exposure observed at the first toxic dose in male rats [45 mg/kg]).

In TDU12766 (single ascending dose), subjects were randomized to receive 2, 5, 15, 25, 50, 100, or 150 mg of venglustat L-malate (providing 1.5, 3.7, 11.2, 18.6, 37.2, 74.4, or 112 mg of free venglustat) or matching placebo in the morning of Day 1 after a \geq 10-hour fast. In FED12767 (food effect), subjects were randomized to receive a single oral dose of 5 mg venglustat L-malate (3.7 mg free venglustat) either while fasting (\geq 10 hours before and 4 hours after administration) or 30 minutes

after a standardized high-fat breakfast (~815 kcal). After a 7-day washout period, participants crossed over to the second period/other condition.

In TDR12768 (multiple ascending doses), subjects were randomized to receive 14 days of once-daily doses of venglustat L-malate 5, 10, or 20 mg (provided as 5-mg capsules; free venglustat doses 3.7, 7.44, or 14.9 mg), or placebo after a ≥ 10 -hour fast.

Assessments

In the single ascending-dose study (TDU12766), blood samples for analysis of plasma venglustat concentrations were collected at 0 (predose), 0.5, 1, 2, 3, 4, 5, 6, 8, 10, 12, 16, 24, 48, 72, and 96 hours postdose. Urine samples were collected for analysis of venglustat concentrations beginning 2 hours before study drug administration through 48 hours afterward.

In the food-effect study (FED12767), blood samples for analysis of plasma venglustat concentrations were collected at 0 pre-dose), 0.5, 1, 2, 3, 4, 5, 6, 8, 10, 12, 16, 24, and 48 hours postdose.

In the repeated ascending-dose study (TDR12768), blood samples for analysis of plasma venglustat concentrations were collected as follows: Day 1: 0 (predose), 0.5, 1, 2, 3, 4, 5, 6, 8, 10, 12, and 16 hours postdose; Days 2–5, 8, 11, and 13: 0 hour (predose); Day 14: 0.5, 1, 2, 3, 4, 5, 6, 8, 10, 12, 24, 48, and 72 hours postdose. Urine samples were collected for analysis of venglustat concentrations on Day 1 (from 2 hours predose to 0 hours postdose) and cumulatively through the dosing interval (0–24 hours postdose) on Day 14. 4 β -Hydroxycholesterol plasma concentrations (to test for induction of CYP3A4,^{21,22} although controversy has developed on the use of this biomarker in the time since our studies were designed) were assessed on Days 1 and 14 (0 hours postdose). Blood samples for PD assessments (plasma GL-1, GL-3, and GM3 concentrations) were collected on Days 1–5, 8, 11, 13, and 14 at 0 hours (predose) and on Day 15, 24 hours after the Day 14 dose. The pharmacodynamic assays used validated liquid chromatography-tandem mass spectrometry (LC-MS/MS) as described elsewhere (GL-1²³; GL-3²⁴) and are summarized in the Supplementary Information, as is the previously unpublished GM3 assay.

Venglustat concentrations in plasma and in urine were determined using their corresponding validated LC-MS/MS methods with a lower limit of quantification (LLOQ) of 0.5 ng/mL for both plasma and urine by QPS, Newark, Delaware. For plasma, the internal standard was Genz-684010 at 20.0 ng/mL; solid-phase extraction of the analyte and internal standard plasma used an Oasis WCX plate, 30 mg/30 μ m. The high-performance liquid chromatography (HPLC) column was Zorbax Bonus-RP, 2.1 \times 50 mm, 1.8 μ m (Agilent, Santa Clara, California), with a mobile phase consist-

ing of A, water:formic acid at 100:0.1 (v:v); B, acetonitrile:formic acid at 100:0.1 (v:v). The gradient started at 95% A, 5% B, ramping to 15% B at 2.5 minutes, 95% B at 2.6–3.0 minutes, then back to 5% B at 3.1 minutes and stopped at 3.12 minutes. Mass spectroscopy used source temperature 600°C; collision gas, 4 pound-force per square inch (psig) N₂; curtain gas, 20 psig N₂; ion source gas 1 and 2, both 50 psig N₂; ion spray voltage, 2000 V; entrance potential, 10 V; and scan duration, 4.0 minutes; monitoring m/z ratios of 390.2 \rightarrow 170.9 for venglustat and 396.2 \rightarrow 226.0 for internal standard. The quantitation range was 0.500 to 500 ng/mL using a 100- μ L sample volume. At 0.500 ng/mL, intraday % coefficient of variation (CV) ranged from 3.8 to 11.6, and intraday % relative error (RE) ranged from -1.4 to -7.6. Between-day variability in LLOQ accuracy was -2.4% RE and in LLOQ precision was 6.7% CV.

Venglustat measurement in urine used 2 methods with different sample volumes and detection ranges. The first (5.0 to 500 ng/mL) used an internal standard of Genz-684010 at 20 ng/mL, with the same solid-phase extraction, HPLC column, and mobile phase as the plasma assay, m/z monitoring at 390.2 \rightarrow 220.0 for venglustat and 396.2 \rightarrow 226.0 for internal standard, had intraday % CV of 4.0 to 5.7, intraday % RE of -4.4 to 3.2, interday % RE of -2.6, and interday % CV of 3.1.

The second urine assay (limit of sensitivity, 5.0–5000 ng/mL) used an internal standard of Genz-684010 at 200 ng/mL and the same solid-phase extraction procedure as for the plasma venglustat assay. The Acquity UPLC (Waters) method, used until 2014, utilized the same HPLC column, mobile phase, and MS settings as for the plasma venglustat assay; m/z ratios monitored were 390.2 \rightarrow 220.0 for venglustat and 396.2 \rightarrow 226.0 for the internal standard. The post-2014 Nexera UHPLC (Shimadzu) method was partially validated from the Acquity method and kept its parameters. Both had limits of sensitivity of 5.00 to 5000 ng/mL and intraday % RE of -2.2.

The plasma 4 β -OH cholesterol assay (used as a marker of CYP3A4 induction or inhibition²³) has an LLOQ of 4 ng/mL and was performed by Bioanalytical Services, Covance Laboratories Ltd., Alnwick, UK. Plasma concentrations and relative actual times were used to calculate pharmacokinetic parameters using validated software (PKDMS, version 2.0 with WinNonlin Professional, version 5.2.1, Certara USA, Inc., Princeton, New Jersey).

The following pharmacokinetic parameters were determined in TDU12766-FED12767: maximum plasma concentration (C_{\max}); time to C_{\max} (t_{\max}); area under the time-concentration curve from $t = 0$ to last measurable concentration (AUC_{last}); AUC extrapolated to infinity (AUC_{inf}); apparent total clearance from plasma

(CL/F); and terminal half-life ($t_{1/2}$). The fraction excreted unchanged in urine through 48 hours (fe_{0-48}) was evaluated in TDU12766 only. Time of last plasma concentration above LLOQ (t_{last}) and time between administration and the sampling time preceding the first concentration above LLOQ (t_{lag}) were determined in FED12767 only. In TDR12768 the following were determined: C_{max} ; trough plasma concentration preadministration (C_{trough}); t_{max} ; AUC over a 24-hour dosing interval (AUC_{0-24}); $t_{1/2}$ (assessed on Day 14); t_{last} ; CL/F at steady state on Day 14 (CL_{ss}/F); fraction excreted unchanged in urine from $t = 0$ to 24 hours after venglustat administration (fe_{0-24}); cumulative amount excreted in urine from $t = 0$ to 24 hours after venglustat administration (Ae_{0-24}); and renal clearance from $t = 0$ to 24 hours after venglustat administration, $CL_{R(0-24)}$.

Pharmacodynamic assessments are described in Supplementary Methods, including details of a plasma GM3 method not previously published (briefly, total GM3 in plasma was quantitated using a protein precipitation procedure followed by LC-MS/MS analysis).

In all studies, safety was evaluated by assessing treatment-emergent adverse events (TEAEs) from first dose through 10 Days after the last dose of study medication, as well as ECG parameters, clinical laboratory values, vital signs, and physical examinations.

Statistical Analyses

Sample sizes for all studies reflected empirical considerations (no sample size calculations were performed). All subjects free of major administration-related deviations (eg, vomiting) were analyzed for pharmacokinetics (TDU12766-FED12767 and TDR12768) and pharmacodynamics (TDR12768). All subjects receiving ≥ 1 dose of venglustat were included in safety analyses. Demographic and baseline characteristics and pharmacokinetic parameters were summarized using descriptive statistics.

For pharmacokinetics, dose effects, food effects, occurrence of steady state, and accumulation were assessed using linear-effects models (Supplementary Methods). The pharmacokinetic parameters shown in Figures 1, 2, and S1 were graphed by regarding values below the LLOQ as zero. For pharmacodynamics, for each parameter (GL-1, GL-3, and GM3), percent reduction from baseline was calculated as (baseline – value/baseline) \times 100. Any pharmacodynamic value below the LLOQ was imputed as LLOQ/2 for consistency with the method used for regulatory-submitted data (and the LLOQ/2 method was used *only* for pharmacodynamic data). For GL-1, the relationship between Day 15 percent reduction from baseline and Day 15 trough concentration was modeled via a sigmoid E_{max} model using the SAS (Statistical Analysis

Software, Cary, North Carolina) NLMIXED procedure,

$$\%reduction = E_0 + (E_{max} \times C^\gamma) (EC_{50}^\gamma + C^\gamma)^{-1}$$

where C is the trough concentration, E_{max} is the maximal percent reduction from baseline, E_0 is the percent reduction from baseline with placebo, EC_{50} is the trough concentration producing half-maximal percent reduction from baseline attributable to venglustat, and γ is a slope parameter.

Trough concentrations for all placebo subjects were set to zero. Model adequacy was assessed graphically by scatterplot of percent reduction from baseline versus trough concentration overlaid with a fitted sigmoid E_{max} model. For each venglustat dose level, the estimated mean percent reduction from baseline attributable to venglustat (with 90% confidence interval [CI]) was calculated from the fitted sigmoid E_{max} model at the corresponding observed geometric mean trough value.

Results

Subject Disposition and Demographics

TDU12766 enrolled and randomized 55 healthy men in the single ascending-dose study (placebo, $n = 14$; 2-, 5-, 15-, 25-, 50-, and 100-mg venglustat L-malate, $n = 6$ each; 150-mg venglustat L-malate, $n = 5$). Eight healthy men participated in the FED12767 food-effect study. TDR12768 (repeated ascending-dose study) enrolled and randomized 36 healthy adults (19 men and 17 women; 4 groups of 9 subjects received placebo or venglustat L-malate 5, 10, or 20 mg). All subjects completed each study; Supplementary Table S1 presents demographics.

Pharmacokinetic Analysis

In the single ascending-dose study (TDU12766), across the single oral doses of venglustat L-malate evaluated (2–150 mg), venglustat was absorbed with a median t_{max} of 3.00 to 5.50 hours and eliminated with a geometric mean $t_{1/2}$ of 28.9 hours (Figure 1B). On Day 14, mean CL/F ranged from 5.18 to 6.43 L/h across the dose groups. Table 1 presents pharmacokinetic parameters following single ascending venglustat doses. Exposure increased close to dose-proportionally throughout the dose range: a 75-fold dose increase resulted in 97.3-, 89.2-, and 85.9-fold increases in geometric mean C_{max} , AUC_{last} , and AUC_{inf} , respectively (Supplemental Table S2). Mean 48-hour urinary excretion fractions were 14.7% to 23.5% over the 2- to 150-mg venglustat L-malate dose range.

In the preliminary assessment of the effect of food on venglustat pharmacokinetics, administration of 5 mg venglustat L-malate with a high-fat meal had no

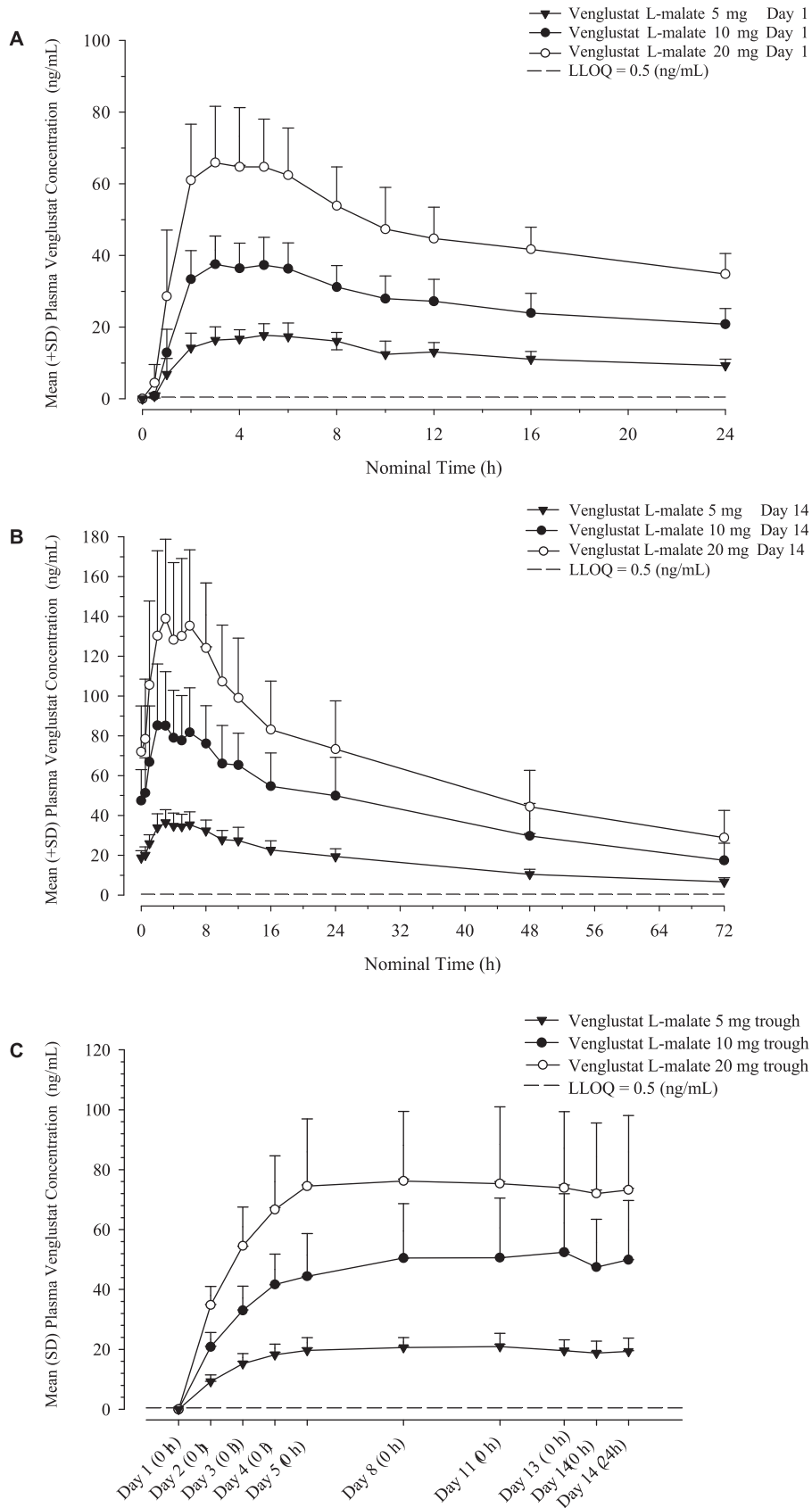


Figure 2. Mean (+ standard deviation) venglustat plasma concentrations on Day 1 (A) and Day 14 (B), and trough concentrations from Day 1 to Day 14 in the repeated ascending-dose study (C). Values below the lower limit of quantitation (LLOQ) were considered zero for this graph

Table 1. Pharmacokinetic Parameters in Single Ascending-Dose Study

Parameter	Oral Venglustat L-Malate Dose							
	2 mg (n = 6)	5 mg (n = 6)	15 mg (n = 6)	25 mg (n = 6)	50 mg (n = 6)	100 mg (n = 6)	150 mg (n = 5)	
C_{max} , ng/mL								
Mean (SD)	5.7 (1.2)	14.7 (1.61)	53.0 (16.7)	84.4 (31.8)	181 (56)	374 (38)	529 (109)	
Geometric mean (CV)	5.6 (21.4)	14.6 (10.9)	50.7 (31.5)	79.9 (37.7)	173 (31)	372 (10.3)	520 (21)	
t_{max} (hours), median (range)	3.50 (3.00–8.00)	5.50 (4.00–8.00)	3.50 (2.00–5.00)	5.00 (4.00–8.00)	4.00 (3.00–6.00)	3.00 (2.00–4.00)	4.00 (1.00–8.00)	
AUC_{last} , ng·h/mL								
Mean (SD)	214 (52)	560 (71)	1830 (520)	3380 (1100)	6310 (1880)	13 000 (2330)	18 600 (5480)	
Geometric mean (CV)	209 (24.3)	556 (12.7)	1760 (29)	3240 (33)	6070 (30)	12 800 (18)	18 000 (30)	
AUC_{inf} , ng·h/mL								
Mean (SD)	243 (61)	652 (122)	2070 (600)	3810 (1080)	7130 (2320)	14 400 (3010)	20 600 (6640)	
Geometric mean (CV)	237 (25)	643 (19)	1990 (29)	3690 (28)	6800 (33)	14 100 (21)	19 900 (32)	
$t_{1/2}$ (hours)								
Mean (SD)	29.2 (43)	33.3 (8.1)	29.7 (7.1)	30.2 (5.5)	28.9 (5.3)	27.8 (3.6)	26.9 (5.7)	
Geometric mean (CV)	28.9 (14.8)	32.5 (24.4)	29.0 (24.0)	29.8 (18.1)	28.5 (18.4)	27.6 (12.8)	26.4 (21.3)	
CL/F, L/h								
Mean (SD)	6.43 (1.41)	5.86 (1.01)	5.85 (1.89)	5.18 (1.31)	5.75 (2.01)	5.38 (1.25)	5.80 (1.55)	
Geometric mean (CV)	6.3 (22.0)	5.8 (17.3)	5.6 (32.2)	5.0 (25.3)	5.5 (34.9)	5.3 (23.4)	5.6 (26.7)	

AUC_{inf} , area under the time-concentration curve extrapolated to infinity; AUC_{last} , AUC from $t = 0$ to last measurable concentration; C_{max} , maximum plasma concentration; CL/F, apparent total clearance from plasma; CV, coefficient of variation; SD, standard deviation; $t_{1/2}$, terminal half-life; t_{max} , time to C_{max} .

Table 2. Pharmacokinetic Parameters on Days 1 and 14 in the Repeated Ascending-Dose Study

Parameter	Venglustat L-Malate Dose		
	5 mg (n = 9)	10 mg (n = 9)	20 mg (n = 9)
C_{max}, ng/mL			
Day 1			
Mean (SD)	18.5 (3.2)	38.5 (7.4)	68.0 (15.7)
Geometric mean (CV)	18.2 (17.3)	37.8 (19.3)	66.5 (23.1)
t _{max} (hours), median (range)	5.00 (2.00–8.17)	3.00 (2.00–5.00)	3.07 (2.00–6.00)
AUC_{0–24}, ng·h/mL			
Mean (SD)	296 (54)	635 (132)	1100 (211)
Geometric mean (CV)	292 (18)	623 (21)	1080 (19)
Day 14			
C_{max}, ng/mL			
Mean (SD)	37.0 (6.4)	89.7 (29.1)	142 (40)
Geometric mean (CV)	36.5 (17.2)	86.0 (32.5)	137 (28.3)
t _{max} (hours), median (range)	3.00 (2.00–6.00)	2.00 (2.00–6.00)	3.00 (2.00–8.00)
AUC_{0–24}, ng·h/mL			
Mean (SD)	642 (121)	1550 (464)	2420 (705)
Geometric mean (CV)	632 (19)	1490 (30)	2340 (29)
C_{trough} (ng/mL)			
Mean (SD)	19.4 (4.0)	49.9 (19.3)	73.3 (24.4)
Geometric mean (CV)	19.0 (20.5)	47.5 (38.7)	69.9 (33.2)
t_{1/2} (hours)			
Mean (SD)	29.3 (4.6)	31.3 (3.3)	35.0 (6.3)
Geometric mean (CV)	29.0 (15.8)	31.2 (10.5)	34.5 (18.0)
CL_{ss}/F (L/h)			
Mean (SD)	5.98 (1.17)	5.13 (1.25)	6.58 (1.70)
Geometric mean (CV)	5.9 (19.5)	5.0 (24.4)	6.4 (25.8)
CL_{R(0–24)} (L/h)			
Mean (SD)	1.55 (0.68)	1.49 (0.41)	2.07 (0.58)
Geometric mean (CV)	NA ^a (44.0)	1.4 (27.7)	2.0 (28.0)

AUC_{0–24}, area under the time-concentration curve over the 24-hour dosing interval; C_{max}, maximum plasma concentration; C_{trough}, trough plasma concentration; CL_{R(0–24)}, renal clearance of venglustat from t = 0 to 24 hours after venglustat dose; CL_{ss}/F, apparent total clearance from plasma at steady state; CV, coefficient of variation; SD, standard deviation; t_{1/2}, terminal half-life; t_{max}, time to C_{max}

^aGeometric mean not calculated because of venglustat concentration below the lower limit of quantification in Day 14 urine sample of 1 subject.

effect on venglustat exposure compared with fasting conditions (Supplemental Tables S3 and S4, Supplemental Figure S1). Fed/fasted geometric mean ratios were 0.92 and 0.91 for C_{max} and AUC_{last}, respectively. Within-subject variability (ie, fed vs fasted) accounted for less than half the total subject variability (Supplemental Table S4). Median t_{max} was 6.00 hours whether fed or fasting (Supplemental Table S3).

In the repeated ascending-dose study (TDR12768) in subjects receiving 5, 10, or 20 mg venglustat L-malate once daily for 14 days, venglustat was absorbed with a median t_{max} of 2.00 to 5.00 hours postdose on Days 1 and 14 (Figure 2A,B). Steady state appeared to be reached within 5 days of repeated dosing (Figure 2C). Table 2 presents pharmacokinetic parameters for all dose groups on Days 1 and 14. Venglustat exposure increased close to dose-proportionally over the dose range of 5–20 mg venglustat L-malate: this 4-fold dose

increase resulted in 3.76- and 3.69-fold increases in geometric mean C_{max} and AUC_{0–24} values, respectively, on Day 14 (Supplemental Table S5). Median and 90th percentile times to steady state are given in Supplemental Table S6. After 14 days of administration, pooled venglustat accumulation ratios were 2.10 for C_{max} and 2.22 for AUC_{0–24}, independent of dose and sex (Supplemental Table S7 and data not shown). Dose and sex also had no effect on t_{1/2} (Supplemental Table S8 and data not shown). Point estimates for within-subject variability were approximately 14% for C_{max} and 13% for AUC_{0–24}. After 14 once-daily doses of venglustat L-malate, the 24-hour unchanged urinary excretion fraction of venglustat (mean fe_{0–24}) ranged between 26.3% and 33.1% (Supplemental Table S9). Mean CL_{R(0–24)} ranged between 1.49 and 2.07 L/h, approximately 3.18- to 3.86-fold lower than observed plasma CL/F. The geometric mean plasma Day 14/Day 1 ratios

Table 3. Point Estimates of Treatment Ratios for Glucosylceramide (GL-1), Globotriaosylceramide (GL-3), and GM3 Ganglioside (GM3) on Day 15 in the Repeated Ascending-Dose Study

Parameter	Comparison	Estimate	90% CI
GL-1	5 mg venglustat L-malate versus placebo	0.39	0.29–0.50
	10 mg venglustat L-malate versus placebo	0.32	0.25–0.42
	20 mg venglustat L-malate versus placebo	0.23	0.17–0.30
GL-3	5 mg venglustat L-malate versus placebo	0.61	0.47–0.79
	10 mg venglustat L-malate versus placebo	0.69	0.53–0.89
	20 mg venglustat L-malate versus placebo	0.67	0.51–0.89
GM3	5 mg venglustat L-malate versus placebo	0.56	0.45–0.70
	10 mg venglustat L-malate versus placebo	0.49	0.39–0.60
	20 mg venglustat L-malate versus placebo	0.40	0.32–0.50

CI, confidence interval.

of 4 β -hydroxycholesterol showed no marked difference between placebo and venglustat-treated groups, indicating minimal induction of CYP3A4 (Supplemental Table S10).

Pharmacodynamic Analyses and Pharmacokinetic/Pharmacodynamic Relationship

In the repeated ascending-dose study (TDR12768), plasma GL-1, GL-3, and GM3 in placebo recipients remained similar to baseline throughout, whereas plasma GL-1 and GM3 levels decreased from baseline time- and dose-dependently across the 3 venglustat dose groups (Table 3, Figure 3).

Maximal sustained effects on GL-1 occurred on Day 11 in the 5- and 10-mg dose groups and by Day 8 in the 20-mg dose group. Mean calculated GL-1 reductions from baseline on Day 15 were 41.9%, 69.6%, and 74.6% in the 5-, 10-, and 20-mg dose groups, respectively. However, these values are mathematically limited by the assay LLOQ and by low baseline GL-1 values relative to the LLOQ, as may be expected in healthy volunteers, who have normal GL-1 levels in plasma. GL-1 values were below the LLOQ at baseline in 1 subject in the 5-mg venglustat L-malate dose group and on Day 15 in 3, 5, and 9 subjects in the 5-, 10-, and 20-mg dose groups, respectively.

Maximal sustained GM3 decreases occurred across all venglustat L-malate dose groups starting on Day 13. Mean Day 15 plasma GM3 levels were 42.7%, 49.4%, and 57.8% of baseline for the 5-, 10-, and 20-mg dose groups, respectively. GM3 was below LLOQ on Day 15 in 1 and 2 subjects in the 10- and 20-mg dose groups, respectively.

Plasma GL-3 also decreased with time in all venglustat L-malate dose groups; however, mean reductions in calculated GL-3 levels are not useful, as GL-3 levels were below the LLOQ at baseline in 11 of 36 subjects enrolled, as may be expected in healthy volunteers who exhibit normal GL-3 levels in plasma.

Mean estimated plasma GL-1 reductions from baseline (90% CI) attributable to venglustat C_{trough} in the 5-, 10-, and 20-mg dose groups (19.0, 47.5, and 69.9 ng/mL, respectively) were 67.0% (54.4%–79.7%), 74.4% (63.7%–85.2%), and 76.3% (64.8%–87.8%), respectively. An E_{max} model adequately described the relationship between venglustat C_{trough} and percent GL-1 reduction (Supplemental Figure S2).

Safety and Tolerability Profile

There were no deaths, serious adverse events (SAEs), severe TEAEs, or TEAEs leading to participant discontinuation reported in any of the 3 studies.

In the single ascending-dose study (TDU12766), 1 subject in the 50-mg dose group and 2 subjects in the 100-mg dose group reported a total of 4 mild TEAEs (Table 4), of which only a headache in 1 subject in the 100-mg dose group on Day 3 was considered study drug-related. In the food-effect study (FED12767), 1 subject reported a mild TEAE in the fed phase of the study (contact dermatitis, reported as “skin irritation at ECG site”), which was considered unrelated to study drug (Table 4).

In the multiple ascending-dose study (TDR12768), 17 subjects reported a total of 32 mild TEAEs, including 10 TEAEs in 6 of 9 subjects (67%) in the placebo group and 22 TEAEs in 11 of 27 total subjects (41%) in the 5-, 10-, and 20-mg dose groups (Table 5). In the venglustat L-malate dose groups, the TEAEs reported by the investigator as study drug-related were constipation, diarrhea, dry mouth, flatulence, pruritus, and fatigue.

No clinically relevant hematologic or biochemical abnormalities were reported in any of the studies. Vital signs and ECG parameters showed no relevant changes from baseline in any of the studies. In the multiple ascending-dose study (TDR12768), no ECG parameters changed statistically significantly from average baseline in any venglustat dose group versus placebo (data not shown).

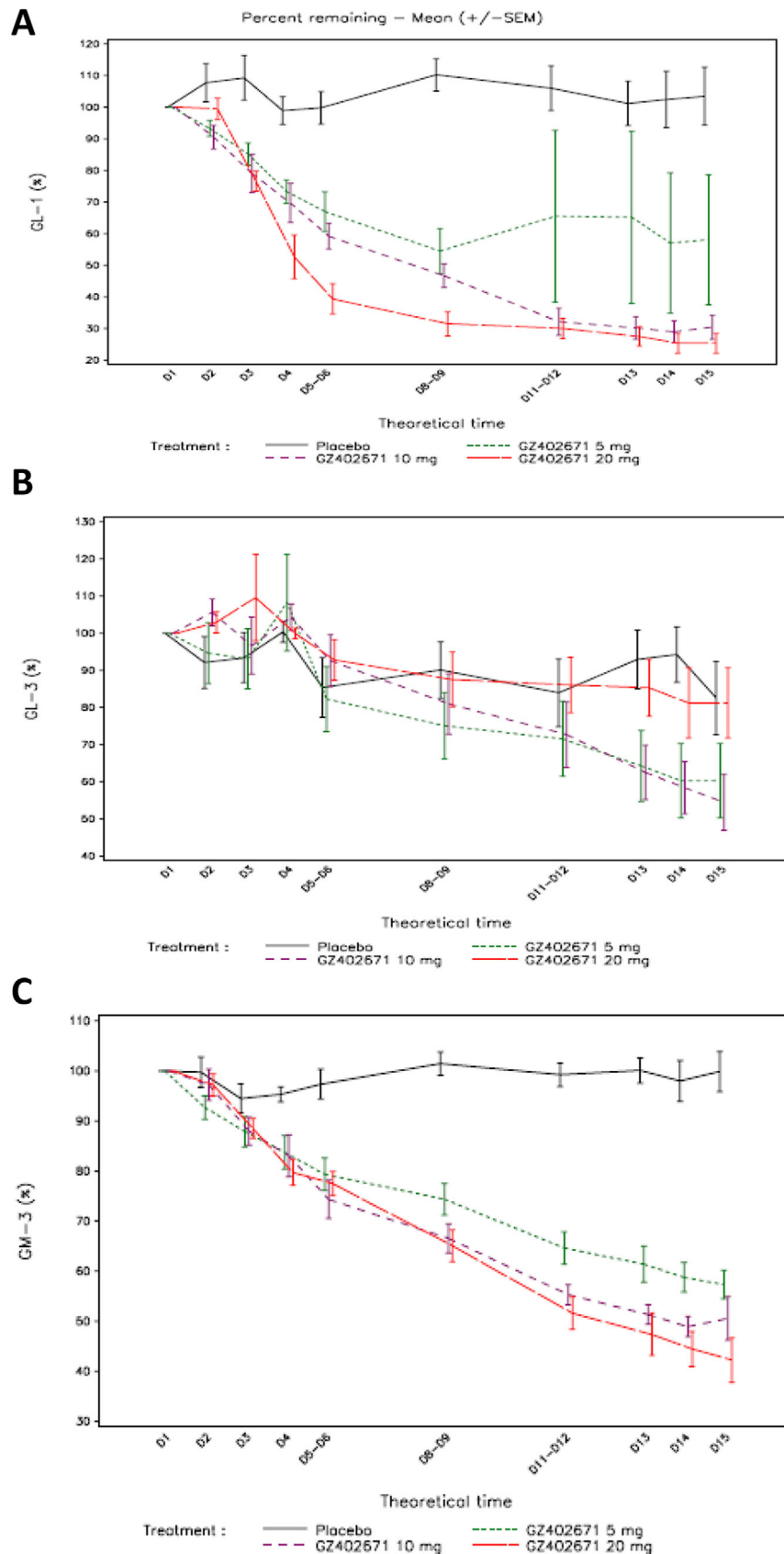


Figure 3. Mean (SEM) remaining of glucosylceramide (GL-1; A), globotriaosylceramide (GL-3; B), and GM3 ganglioside (GM3; C) in placebo, 5-, 10-, and 20-mg dose groups (venglustat L-malate, GZ402671) from Day 1 to Day 15 in the repeated ascending-dose study

Table 4. Treatment-Emergent Adverse Events (TEAEs) in the Single Ascending-Dose and Food-Effect Studies

TEAE, n (%) Primary System Organ Class ^a Preferred Term ^a	Venglustat L-Malate Dose Groups						
	Placebo (n = 14)	Single Ascending-Dose Study				Food-Effect Study	
		2-25 mg ^b (n = 24)	50 mg (n = 6)	100 mg (n = 6)	150 mg (n = 5)	5 mg fed (n = 8)	5 mg fasted (n = 8)
Any TEAE	0	0	1 (16.7)	2 (33.3)	0	1 (12.5)	0
Skin and subcutaneous tissue disorders	0	0	0	1 (16.7)	0	1 (12.5)	0
Dermatitis contact	0	0	0	1 (16.7)	0	1 (12.5)	0
Infections and infestations	0	0	1 (16.7)	0	0	0	0
Rhinitis	0	0	1 (16.7)	0	0	0	0
Nervous system disorders	0	0	0	1 (16.7)	0	0	0
Headache	0	0	0	1 (16.7)	0	0	0
General disorders and administration-site conditions	0	0	1 (16.7)	0	0	0	0
Feeling cold	0	0	1 (16.7)	0	0	0	0

^aPer the Medical Dictionary for Regulatory Activities, version 15.1.

^bPooled data for dose groups.

Table 5. Treatment-Emergent Adverse Events (TEAEs) in the Repeated Ascending-Dose Study

TEAE, n (%) Primary System Organ Class ^a Preferred Term ^a	Venglustat L-malate Dose Groups			
	Placebo (n = 9)	5 mg (n = 9)	10 mg (n = 9)	20 mg (n = 9)
Any TEAE	6 (66.7)	3 (33.3)	4 (44.4)	4 (44.4)
Skin and subcutaneous tissue disorders	1 (11.1)	2 (22.2)	3 (33.3)	1 (11.1)
Dermatitis contact	1 (11.1)	0	1 (11.1)	1 (11.1)
Pruritus	0	1 (11.1)	0	0
Skin irritation	0	2 (22.2)	2 (22.2)	0
Gastrointestinal disorders	1 (11.1)	1 (11.1)	1 (11.1)	3 (33.3)
Diarrhea	1 (11.1)	0	1 (11.1)	1 (11.1)
Dry mouth	0	0	0	1 (11.1)
Flatulence	0	0	0	1 (11.1)
Constipation	1 (11.1)	1 (11.1)	1 (11.1)	0
Respiratory, thoracic and mediastinal disorders	1 (11.1)	1 (11.1)	0	2 (22.2)
Nasal congestion	0	0	0	2 (22.2)
Oropharyngeal pain	1 (11.1)	0	0	0
Rhinitis allergic	0	1 (11.1)	0	0
Nervous system disorders	4 (44.4)	0	0	1 (11.1)
Headache	3 (33.3)	0	0	1 (11.1)
Dizziness postural	1 (11.1)	0	0	0
Infections and infestations	2 (22.2)	0	0	1 (11.1)
Upper respiratory tract infection	0	0	0	1 (11.1)
Nasopharyngitis	1 (11.1)	0	0	0
Sinusitis	1 (11.1)	0	0	0
Musculoskeletal and connective tissue disorders	0	0	1 (11.1)	0
Neck pain	0	0	1 (11.1)	0
General disorders and administration-site conditions	0	0	0	1 (11.1)
Fatigue	0	0	0	1 (11.1)

^aPer the Medical Dictionary for Regulatory Activities, version 15.1.

Discussion

Phase 1 studies were conducted with venglustat in healthy male and female volunteers. The objectives of these studies were to determine the pharmacokinetics, and pharmacodynamics, safety tolerability of orally administered venglustat L-malate and to assess the effect of food on venglustat pharmacokinetics. The main goal of the studies was to determine doses of venglustat with favorable safety and tolerability that could be tested in subsequent trials.

In these phase 1 studies, venglustat demonstrated linear pharmacokinetics (when administered as single venglustat L-malate doses ranging from 2 to 150 mg or as repeated once-daily doses ranging from 5 to 20 mg for 14 days), rapid absorption, systemic exposure unaffected by food, low apparent total body clearance, and mean fraction of dose excreted unchanged in urine (f_{e0-24}) ranging from 26.3% to 33.1%.

Plasma pharmacodynamic evaluation following repeated once-daily doses of venglustat demonstrated reduction of plasma concentrations of GL-1 and GM3 in a time- and dose-dependent manner, consistent with its proposed mechanism of action: venglustat-mediated GCS inhibition. The effect of venglustat on GL-3 was not testable in this study, as the baseline levels of GL-3 in healthy volunteers were below the LLOQ. The dose- and time-dependent GL-1 and GM3 reductions corroborated the intended mechanism of action of venglustat: decreased GL-1 formation via inhibition of GCS and the resulting decreased downstream GM3 formation.

Modeling of pharmacokinetic-pharmacodynamic relations indicated an E_{max} of 80% for venglustat, which was closely approached following administration of 20 mg venglustat L-malate in the repeated-dose study (mean GL-1 reduction from baseline on Day 15, 74.6%).

At the doses and dosing regimen tested, venglustat showed a favorable safety and tolerability profile. First-in-human healthy-volunteer studies support the conduct of subsequent studies in patients with targeted diseases, but do not necessarily predict their safety or pharmacokinetic results. Nonetheless, in a 2019 presentation to the American Association of Neurology, MOVES-PD Part 1 participants with *GBA*-PD receiving venglustat for 26 weeks demonstrated no SAEs or deaths, near-dose-proportional plasma and cerebrospinal fluid pharmacokinetics, and dose-dependent GL-1 and GL-3 reduction.^{20,25} A full article on that study is in preparation.

Conclusions

In 3 phase 1 studies in healthy subjects, at the doses and dosing regimen tested, venglustat showed a safety and tolerability profile without SAEs or severe

adverse events. Repeated once-daily venglustat dosing up to 20 mg venglustat L-malate for 2 weeks (corresponding to 15 mg venglustat) reduced plasma GL-1 concentrations in a time- and dose-dependent manner. Steady-state plasma concentrations of venglustat occurred within 5 days of repeated dosing, with an approximately 2-fold accumulation ratio for C_{max} and AUC_{0-24} and a near-dose-proportional increase in exposure.

The pharmacokinetic, pharmacodynamic, and safety and tolerability results of the phase 1 studies support clinical development of venglustat as an oral GCS inhibitor in phase 2 and phase 3 studies designed to test the hypothesis that GL-1 is a key node for pathophysiology in diverse diseases involving the glycosphingolipid pathway.

Acknowledgments

This study was supported by Sanofi Genzyme. Editorial support in the preparation of this publication was provided by Kim Coleman Healy, PhD, CMPP, of Elevate Medical Affairs, contracted by Sanofi Genzyme for publication support services. The authors, individually and collectively, are responsible for all content and editorial decisions and received no payment from Sanofi directly or indirectly (through a third party) related to the development/presentation of this publication.

Conflicts of Interest

M.J.P., S.J.M.G., A.J.J., and J.S. are full-time employees of Sanofi Genzyme. N.P.S.C. was a Sanofi employee at the time of the studies. T.T.P. is a full-time employee of PPD Development, LLC, contracted by Sanofi Genzyme to perform the studies.

Funding

These studies were supported by Sanofi Genzyme.

Data Sharing

Qualified researchers may request access to patient-level data and related study documents including the clinical study report, study protocol with any amendments, blank case report form, statistical analysis plan, and data set specifications. Patient-level data will be anonymized, and study documents will be redacted to protect the privacy of trial participants. Further details on Sanofi's data sharing criteria, eligible studies and process for requesting access can be found at: <https://www.clinicalstudydatarequest.com>.

References

1. Shayman JA. Targeting glucosylceramide synthesis in the treatment of rare and common renal disease. *Semin Nephrol.* 2018;38(2):183-192.

2. Hannun YA, Obeid LM. Sphingolipids and their metabolism in physiology and disease. *Nat Rev Mol Cell Biol.* 2018;19(3):175-191.
3. Kolter T, Sandhoff K. Sphingolipid metabolism diseases. *Biochim Biophys Acta.* 2006;1758(12):2057-2079.
4. Baris HN, Cohen IJ, Mistry PK. Gaucher disease: the metabolic defect, pathophysiology, phenotypes and natural history. *Pediatr Endocrinol Rev.* 2014;12(suppl 1):72-81.
5. Bokhari SRA, Zulfikar H, Hariz A. Fabry disease. *StatPearls.* Treasure Island, FL; 2020 Sept 8.
6. Cachon-Gonzalez MB, Zaccariotto E, Cox TM. Genetics and therapies for GM2 gangliosidosis. *Curr Gene Ther.* 2018;18(2):68-89.
7. Gegg ME, Schapira AHV. The role of glucocerebrosidase in Parkinson disease pathogenesis. *FEBS J.* 2018;285(19):3591-3603.
8. Chatterjee S, Shi WY, Wilson P, Mazumdar A. Role of lactosylceramide and MAP kinase in the proliferation of proximal tubular cells in human polycystic kidney disease. *J Lipid Res.* 1996;37(6):1334-1344.
9. Deshmukh GD, Radin NS, Gattone VH, 2nd, Shayman JA. Abnormalities of glycosphingolipid, sulfatide, and ceramide in the polycystic (cpk/cpk) mouse. *J Lipid Res.* 1994;35(9):1611-1618.
10. Natoli TA, Husson H, Rogers KA, et al. Loss of GM3 synthase gene, but not sphingosine kinase 1, is protective against murine nephronophthisis-related polycystic kidney disease. *Hum Mol Genet.* 2012;21(15):3397-3407.
11. Natoli TA, Smith LA, Rogers KA, et al. Inhibition of glucosylceramide accumulation results in effective blockade of polycystic kidney disease in mouse models. *Nat Med.* 2010;16(7):788-792.
12. Coutinho MF, Santos JJ, Matos L, Alves S. Genetic substrate reduction therapy: a promising approach for lysosomal storage disorders. *Diseases.* 2016;4(4):33.
13. Stirnemann J, Belmatoug N, Camou F, et al. A review of Gaucher disease pathophysiology, clinical presentation and treatments. *Int J Mol Sci.* 2017;18(2):441.
14. Lukina E, Watman N, Arreguin EA, et al. A phase 2 study of eliglustat tartrate (Genz-112638), an oral substrate reduction therapy for Gaucher disease type 1. *Blood.* 2010;116(6):893-899.
15. Sardi SP, Viel C, Clarke J, et al. Glucosylceramide synthase inhibition alleviates aberrations in synucleinopathy models. *Proc Natl Acad Sci U S A.* 2017;114(10):2699-2704.
16. Marshall J, Sun Y, Bangari DS, et al. CNS-accessible inhibitor of glucosylceramide synthase for substrate reduction therapy of neuronopathic Gaucher disease. *Mol Ther.* 2016;24(6):1019-1029.
17. Ashe KM, Budman E, Bangari DS, et al. Efficacy of enzyme and substrate reduction therapy with a novel antagonist of glucosylceramide synthase for Fabry disease. *Mol Med.* 2015;21(1):389-399.
18. Schiffmann R, Mengel E, Crawford N, et al. Venglustat in adult Gaucher disease type 3: Preliminary safety, pharmacology, and exploratory efficacy from a phase 2 trial in combination with imiglucerase (LEAP) [Abstract 320, WORLD 2019]. *Mol Genet Metab.* 2019;126(2):S131.
19. Aflaki E, Westbroek W, Sidransky E. The complicated relationship between Gaucher disease and Parkinsonism: Insights from a rare disease. *Neuron.* 2017;93(4):737-746.
20. Peterschmitt MJ, Gasser T, Isaacson S, et al. Safety, tolerability and pharmacokinetics of oral venglustat in Parkinson disease patients with a *GBA* mutation [Abstract, WORLD 2019]. *Mol Genet Metab.* 2019;126(2):S117.
21. Kasichayanula S, Boulton DW, Luo WL, et al. Validation of 4beta-hydroxycholesterol and evaluation of other endogenous biomarkers for the assessment of CYP3A activity in healthy subjects. *Br J Clin Pharmacol.* 2014;78(5):1122-1134.
22. Mao J, Martin I, McLeod J, et al. Perspective: 4beta-hydroxycholesterol as an emerging endogenous biomarker of hepatic CYP3A. *Drug Metab Rev.* 2017;49(1):18-34.
23. Ji AJ, Wang H, Ziso-Qejvanaj E, et al. A novel approach for quantitation of glucosylceramide in human dried blood spot using LC-MS/MS. *Bioanalysis.* 2015;7(12):1483-1496.
24. Roddy TP, Nelson BC, Sung CC, et al. Liquid chromatography-tandem mass spectrometry quantification of globotriaosylceramide in plasma for long-term monitoring of Fabry patients treated with enzyme replacement therapy. *Clin Chem.* 2005;51(1):237-240.
25. Fischer T, Gasser T, Isaacson S, et al. Safety, tolerability and pharmacokinetics of oral venglustat in Parkinson's disease patients with a *GBA* mutation (S4.002). *Neurology.* 2019;92(suppl 15):S4.002.

Supplemental Information

Additional supplemental information can be found by clicking the Supplements link in the PDF toolbar or the Supplemental Information section at the end of web-based version of this article.